frequency sensitivity can be expressed as

$$S_{\text{sq law}} = \left.\frac{dV_{op}}{dw}\right|_{w=w_0} = (-1)^n \eta_1 V_0^2 (2n+1)\pi/(2w_0 g_1).$$

The frequency response characteristics of the discriminator under square law operation of the AM detectors is shown in Fig. 6. The length of the waveguide line used in the experiment is measured to be 28.6 cm·s. The corresponding value of "$n$" when calculated is 18. The sensitivity of this discriminator is found to be 5.7 mV/MHz for an input power level of 8 mW. The center frequency of this discriminator is 9.356 GHz and the peaks in the frequency response appear for frequency deviations of $\pm 68$ MHz theoretically. Discriminator output as measured from a dual-trace oscilloscope is 250 mV at the response peaks. The measured output voltages are divided by a factor of 250 in order to normalize the response to a maximum value of unity.

Assuming linear operation of the envelope detectors, it is seen that the discriminator cannot be implemented with the difference in lengths of the shorted waveguides corresponding to the odd integral values of "$n$." The discriminator implemented with an even integral "$n$" possesses only odd harmonic distortion at its output. Fig. 5 shows that the third harmonic distortion in square law operation is higher than that in linear operation. Peaks in the frequency response occur for $\Delta w/w_0 = \pm 2g_1/(2n+1)$. The discriminator sensitivity in linear operation is given by

$$S_{\text{lin}} = (-1)^{n/2} \eta_2 V_0 (2n+1)\pi/(2\sqrt{2}\, w_0 g_1).$$

## IV. Experiment

A schematic diagram of the experimental setup is shown in Fig. 1. The tunable high-$Q$ Gunn oscillator (0902 EC X-480B) using Microwave Associates' Gunn diode (No. MA 49104) served as the source of coherent carrier. The Marconi AM–FM signal source (Model 6158A) having a frequency modulation sensitivity of 2 MHz/V and a maximum frequency modulation rate of 0.1 MHz is used as the FM generator. Any reflection from the detector connected with the $E$-arm of the magic tee is eliminated by the isolator preceding it. The lockband of the oscillator is reduced sufficiently by attenuating the strength of the synchronizing signal. The $Q$-factor and the free-running output power of the Gunn oscillator are 2198 and 58 mW, respectively. Total lockband of the Gunn oscillator is 0.25 MHz for a CW injection power of 0.2 mW at 9.356 GHz.

## V. Discussion and Conclusion

Symmetrical tuning of the adjustable diode detectors is very important for producing maximum linearity in the response of the discriminator. A high-$Q$ passive resonant cavity tuned at the FM carrier frequency can be placed before the narrow-band Gunn oscillator in order to achieve a better sideband suppression. Low index, fast modulation is preferred for this technique since low index of modulation produces less harmonic distortion at the discriminator output, while fast modulation produces strong sideband suppression.

## References


[1] R. V Pound, "Electronic frequency stabilization of microwave oscillators," *Review of Scientific Instruments*, vol. 17, pp 490–505, Nov 1946.

[2] C. K Chan and R S. Cole, "A stable microwave integrated circuit X-band Gunn oscillator," *IEEE Trans. Microwave Theory Tech.*, p. 815, Aug. 1974.

[3] C. W. Lee and W. Y. Seo, "Super wide-band FM line discriminator," *Proc. IEEE*, pp. 1675–1676, Nov. 1963

[4] C. W Lee, "An analysis of a super wide-band FM line discriminator," *Proc. IEEE*, pp. 1034–1038, Sept 1964.

[5] R J. Mohr, "Broad-band microwave discriminator," *IEEE Trans Microwave Theory Tech.*, pp. 263–264, July 1963

[6] S J. Robinson, "Comment on broad-band microwave discriminator," *IEEE Trans on Microwave Theory Tech.*, pp 255–256, Mar 1964.

[7] E. H. Katz and H. H. Schreiber, "Design of phase discriminators," *Microwaves*, pp 26–33, Aug 1965.

[8] L. I Reber, "Improved performance in phase discriminators," *Microwaves*, pp. 48–52, May 1971

[9] M L Sisoida and O. P. Gandhi, "Octave bandwidth *L*- and *S*-band stripline discriminators," *IEEE Trans Microwave Theory Tech.*, pp 271–272, Apr. 1967

[10] S. R Mishra and R P Wadhwa, "Development of an *X*-band waveguide frequency discriminator," *IEEE Trans. Microwave Theory Tech.*, pp. 660–661, Sept 1970.

[11] W Y Seo, "Microwave discriminator for above 10 Gc," *Proc. IEEE*, p. 179, Feb. 1965.

[12] R. L Addington, "Comments on 'microwave discriminator for above 10 Gc' & 'stripline phase shifter,'" *Proc. IEEE*, p 1229, Sept. 1965

[13] J Nigrin, N. A Mansour, and W. A. G Voss, "Single hybrid tee frequency discriminator," *IEEE Trans. Microwave Theory Tech.*, pp 776–778, Sept. 1975

[14] P. Z. Peebles, Jr and A H. Green, "A microwave discriminator with easily adjusted bandwidth," in *Proc. of Southeast Conf.*, Roanoke, VA, 1979, pp. 275–277

[15] P Z. Peebles, Jr. and A. H Green, Jr., "A microwave discriminator at 35 GHz," *Proc IEEE*, pp. 286–288, Feb 1980.

[16] B. Glance, "Digital phase demodulator," *Bell Syst. Tech. J*, pp. 933–949, Mar 1971


# New Concepts in Traveling-Wave Amplifiers

M. FRIEDGUT

*Abstract*—**Two new networks with the potential for good port VSWR over very broad bandwidths are proposed for use in both low-power balanced amplifiers, and high-power combining systems. These new structures which are called Low-Sidelobe and Squintless Traveling-Wave Amplifiers (LSTWA and SQTWA, respectively) have been derived from conventional Traveling-Wave Amplifiers (TWA) by utilizing Phased Array Antenna concepts and design techniques. Using Monte-Carlo simulations the relative performance of the three structures is compared. Finite loss and mismatch effects are also considered.**

## I. Introduction

Wide bandwidth requirements in low-noise/low-power amplifiers have generally been met by using multisection Lange couplers to realize cascadable low VSWR-balanced modules. Active devices covering the full 2–20 GHz frequency range are routinely available today [1] and thus the coupler performance is often the limiting factor in such designs [2].

High-power requirements over wide bands on the other hand, generally lead to the use of combiner networks to achieve the desired power levels [3], [4]. In monolithic designs, the traveling-wave structure [5] is a promising contender.

In the following sections, the conventional TWA is compared with the LSTWA and SQTWA structures. Design and analysis methods from Phased Array theory provide insight into the combining and matching properties of all these devices.

In Section II, expressions will be developed for the input reflection-coefficient and forward transmission coefficient for the

Manuscript received January 18, 1985; revised November 18, 1985

The author is with AWA Communications Laboratory, North Ryde, 2113, N.S W Australia

IEEE Log Number 8407187

three devices. The general case which includes both loss and mismatch effects is developed, and simplified models are also derived to illustrate the fundamental differences between the structures. Section III presents comparative simulation results, Section IV contains discussion of these results, and Section V is the conclusion.

## II. Comparative Analysis

A typical configuration for a general 4-element TWA is shown in Fig. 1.

The amplifier may be visualized as consisting of five cascaded blocks:

i) an equiphase divider block (INPUT) to plane $A-A'$);
ii) a phase tilt block ($A-A'$ to $B-B'$);
iii) an active device block ($B-B'$ to $C-C'$);
iv) an inverse phase tilt block ($C-C'$ to $D-D'$);
v) an equiphase combiner block ($D-D'$ to OUTPUT).

Using $S$ parameters [6], block (i) is represented by ($S'$), block (ii) by ($S''$), and block (iii) by ($S'''$). Assuming that the reverse transmission of the active devices is small, and that passive device mismatch levels are reasonably low, then the overall TWA INPUT reflection-coefficient $\Gamma i$ is given by:

$$\Gamma i = S'_{11} + S'_{12}S''_{11}\{1-S'_{22}S''_{11}\}^{-1}S'_{21} + S'_{12}\{1-S''_{11}S'_{22}\}^{-1}S''_{12}S'''_{11} \cdot\left(1-\left[\{S''_{22}+S''_{21}S'_{22}\{1-S''_{11}S'_{22}\}^{-1}S''_{12}\}\{S'''_{11}\}\right]\right)^{-1} \cdot S''_{21}\{1-S'_{22}S''_{11}\}^{-1}S'_{21}. \quad (1)$$

If block (iv) is represented by ($S^{\mathrm{iv}}$) and (v) by ($S^{\mathrm{v}}$), then the overall forward transmission coefficient $T_f$ is given by:

$$T_f = S^{\mathrm{v}}_{21}\{1-S'''_{22}S^{\mathrm{v}}_{11}\}^{-1}S^{\mathrm{iv}}_{21}\{1-S'''_{22}S^{\mathrm{iv}}_{11}\}^{-1}S'''_{21} \cdot\left(1-\left[\{S''_{22}+S''_{21}S'_{22}\{1-S''_{11}S'_{22}\}^{-1}S''_{12}\}\{S'''_{11}\}\right]\right)^{-1} \cdot S''_{21}\{1-S'_{22}S''_{11}\}^{-1}S'_{21}. \quad (2)$$

By algebraic manipulation, these equations may be reduced to the following forms:

$$\Gamma i = K_1\angle k_1 + X\sum_{n=o}^{3}|C_n||S'''_{11_n}|A_n^2\exp\{-nLl\} \cdot\exp\left\{j\left(n\angle 2\psi^f + \angle c_n + \angle S'''_{11_n}\right)\right\} \quad (3)$$

$$T_f = X\sum_{n=0}^{3}|C_n||S'''_{21_n}|A_n^2\exp\left\{j\left(3n\psi^f + \angle c_n + \angle S'''_{21_n}\right)\right\} \quad (4)$$

where

$X$ symmetric loss term,*
$L$ non symmetric loss term,**
$K_1\angle k_1$ complex additive term with magnitude $|K_1|$ and phase $\angle k_1$ resulting from mismatch at INPUT, OUTPUT, planes $A-A'$, and $D-D'$,
$C_n\angle c_n$ complex multiplicative mismatch term,
$\psi^f$ one-way phase contribution of network $\zeta$ in Fig. 1,
$A_n$ scalar amplitude weighting in channel $n$,
$j$ $\sqrt{-1}$.

Notes

* the loss component which is equal in all channels,
** the loss component which differs in adjacent channels by the factor $n$.

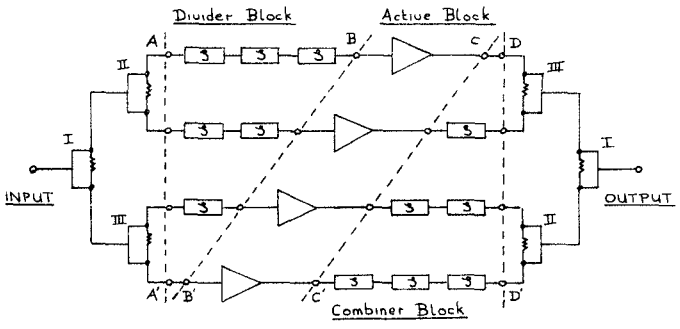


Fig. 1. General TWA.

In order to illustrate the basic behavior of the TWA, LSTWA, and SQTWA, it is useful to study simpler expressions which highlight the essential differences. If blocks (i), (ii), (iv), and (v) are perfectly matched, then (1) and (2) may be simplified as follows:

$$\Gamma i \sim S'_{12}S''_{12}S'''_{11}S''_{21}S'_{21} \quad (5)$$

$$T_f \sim S^{\mathrm{v}}_{21}S^{\mathrm{iv}}_{21}S'''_{21}S''_{21}S'_{21} \quad (6)$$

which may also be expressed as follows:

$$\Gamma_i \sim \sum_{n=0}^{3}|S'''_{11_n}|A_n^2\exp\left\{j\left(n\angle\psi^f + \angle S'''_{11_n}\right)\right\} \quad (7)$$

$$T_f \sim \sum_{n=0}^{3}|S'''_{21_n}|A_n^2\exp\left\{3j\psi^f + \angle S'''_{21_n}\right\}. \quad (8)$$

### A. The TWA

In Figure 1. consider network $\zeta$ to be a matched delay line of length $l$ (permittivity $\epsilon=1$ for convenience) and splitters I, II, and III to be equal amplitude/phase types (i.e., $A_i=1/\sqrt{4}$ in (7)). In this case a unit amplitude signal at the TWA INPUT results of equal amplitude at plane $B-B'$, but whose phase between adjacent channels differs by $\psi^f$ where

$$\psi^f = 2\pi l/\lambda. \quad (9)$$

Note that $\lambda$ is wavelength (recall that $\epsilon=1$).

These signals are reflected at the active device plane ($B-B'$ at a level determined by ($S'''_{11}$) and the resultant backward signals at plane $A-A'$ have equal amplitudes, but phase increments between adjacent channels given by $\psi^r$ where

$$\psi^r = 2\psi^f. \quad (10)$$

These signals are summed in a vector fashion by the splitters, and the resultant INPUT reflection-coefficient is given by (7). This equation is seen to be similar to that describing the far-field radiation pattern of a Linear Phased Array [7]:

$$A = \sum_{n=0}^{3}|W_n|\exp\{jn(kd\sin\theta+\gamma)\} \quad (11)$$

where

$A$ far-field radiation pattern amplitude,
$W_n$ element scalar weight,
$k$ $2\pi/\lambda$,
$d$ interelement spacing,
$\gamma$ element weighting phase,
$\theta$ spatial angle.

### B. The LSTWA

The similarity between (7) and (11) suggests that Phased Array low-sidelobe techniques may be applied to advantage in the TWA structure in order to lower the level of $\Gamma_t$. One such technique is amplitude distribution tapering [8] which modifies the $A_t$ in (7). This type of distribution may be realized in lossless form by using unequal power splitters [9] or directional couplers for splitters II and III in Fig. 1.

In order to maintain lossless forward transmission, the $A_t$ must satisfy the following condition:

$$\sum_{n=0}^{3} (A_t)^2 = 1. \tag{12}$$

### C. The SQTWA

Again drawing on analogies with Phased Arrays, it is seen from (9) and (10) that the behavior of $\Gamma_t$ in (7) for the TWA is reminiscent of the phenomenon of beam squint [10].

If the networks $\zeta$ in Fig. 1 are changed from matched delay lines (as in the TWA and LSTWA) to matched wide-band fixed shifters [11], then $\psi^r$ is given by:

$$\psi^r = \Phi \tag{13}$$

where $\Phi$ may be chosen arbitrarily, and is not frequency-dependent (within the phase shifters design bandwidth of course). Note that in the SQTWA, splitters I, II, and III are all equal amplitude/phase types, and so all $A_t$ are equal ($=1/\sqrt{4}$).

If $\Phi$ is chosen so that the form under the summation in (7) adds up to zero, then $\Gamma_t$ is zero as long as the splitters and phase shifters are within their operating bandwidths. Since both power splitters [12] and fixed phase shifters [11] may be designed for operating bandwidths of at least 10:1, this is the potential operating bandwidth of the SQTWA.

### D. Design Rules

The frequency-dependent behavior of $\Gamma t$ for the TWA and LSTWA results from the vector rotation caused by the frequency dependence of $\psi^l$ in (7). For maximum bandwidth performance, the length $l$ of the delay line $\zeta$ at the design center frequency is given by:

$$l = \lambda/4. \tag{14}$$

In the SQTWA, the vectors do not rotate, but are displaced from each other by multiples of $2\Phi$, and $\Gamma_t$ may be set equal to zero using the following relationship:

$$\Phi = \pi m/M \tag{15}$$

where

$M$ no. of elements (4 in this example),
$m$ an integer $1, 2, \cdots, M-1$.

### E. Forward Transmission

From (8) it is seen that the vectors are coincident for the TWA, LSTWA, and SQTWA, irrespective of the nature of $\psi^l$, and as such $T_f$ is independent of frequency.

## III. Simulation Results

The previous sections consider the relative behavior of the TWA, LSTWA, without taking into account finite component tolerances. In this section, $(S_{11}''')_n$ and $(S_{21}''')_n$ (i.e., the input reflection-coefficients and forward transmission coefficients, respectively) of the active devices are allowed to vary at random within specific limits.

### A. Combining Performance

From (4) and (8) it is clear that $T_f$ has a maximum value of $S_{21}'''$. Thus all tolerance, matching, and loss effects act to reduce this value, which yields a power gain given by:

$$G = |T_f|^2 = |S_{21}'''|^2. \tag{16}$$

Simulations are performed for $T_f$ under the following conditions:

*Case (a)* Active device $(S_{11}''')i$ and $(S_{21}''')i$ parameter variations of $\pm 3$ percent, $\pm 10$ percent in amplitude, and $\pm 10°$, $\pm 20°$ in phase. All passive components are lossless and perfectly matched.

Case (b) Active device $(S_{11}''')i$ and $(S_{21}''')i$ parameter variations of $\pm 10$ percent in amplitude, $\pm 20°$ in phase, and passive components lossless with matching return loss levels of $-15$ dB.

Since path lengths are equal for all channels, component losses may be designed to be equal in each channel, and thus loss appears outside the summation $X$ in (4). Therefore, component losses are simply additive. Table I in Section IV presents the simulation results for forward transmission of the overall TWA's.

### B. INPUT Port Return Loss Performance

In this section, four simulations are described. The first (called the zero-tolerance case) considers identical active devices, and perfectly matched, lossless passive components.

The second and third simulations (called non-zero tolerance cases) consider active devices with $S$ parameter spreads of $\pm 10$ percent in amplitude, and $\pm 10°$, $\pm 20°$ in phase, respectively. Passive components are still taken to be lossless and perfectly matched. The final simulation (called the mismatched case) considers $\pm 10$ percent, $\pm 20°$ active device amplitude/phase variations, passive device mismatch return loss levels of $-15$ dB, and an unsymmetric loss term of $1\text{dB}/\lambda$ at the center frequency.

This center frequency has been chosen at 9GHz, and the nominal active device $(S_{11}''')$ set at 0.9.

Active device parameter variations are simulated using Monte-Carlo analysis, with amplitude and phase being allowed to vary independently within a specified window.

Passive divider/combiner weighting coefficients for the LSTWA were chosen to yield sidelobes of $-20$ dB ([8] p. 147) as follows:

$$A_1 = A_2 = \sqrt{.31}$$
$$A_0 = A_3 = \sqrt{.19}. \tag{17}$$

The fixed phase shifters for the SQTWA were chosen according to (15) with $M = 4$ and $m = 2$

Figs. 2–5 and Table II in Section IV show the results of the four simulations described above, for INPUT Port Return Loss.

## IV Discussion

### A. Forward Transmission

Table I presents comparative results for the simulations described in Section III-A.

In general, for the cases considered, the combining performance for the TWA, LSTWA, and SQTWA are very similar. Thus the choice of structure may be based on the difference in the behavior of $\Gamma_t$, which is described in the next section.

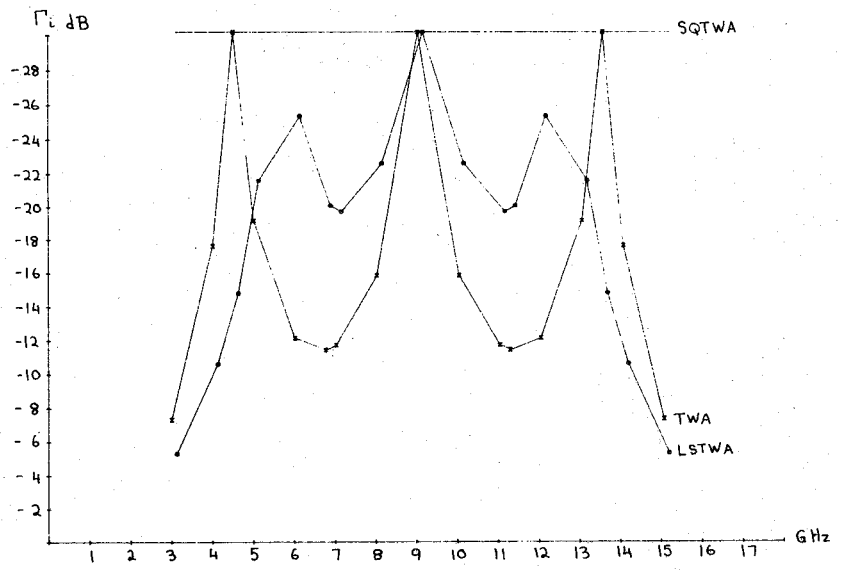


Fig. 2. INPUT port return loss (zero-tolerance case).

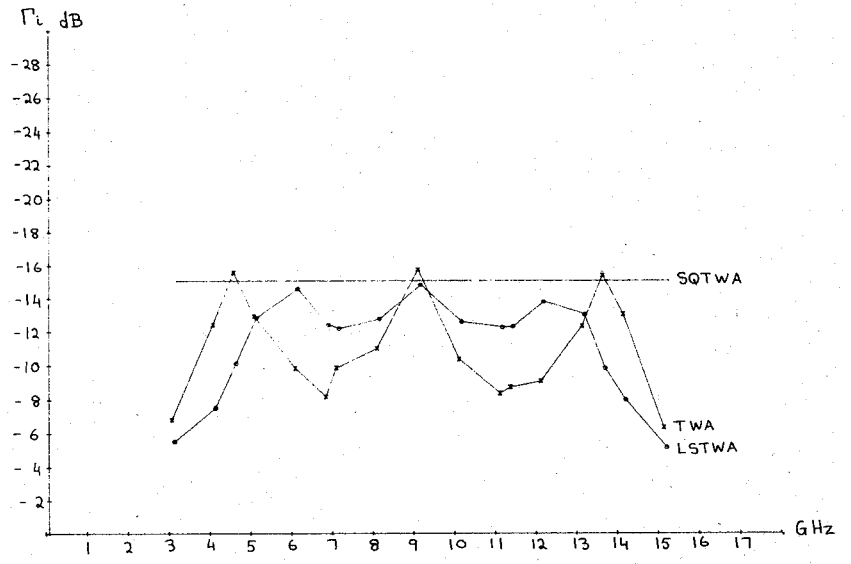


Fig. 3. INPUT port return loss (nonzero-tolerance, ±10 percent, ±10°).

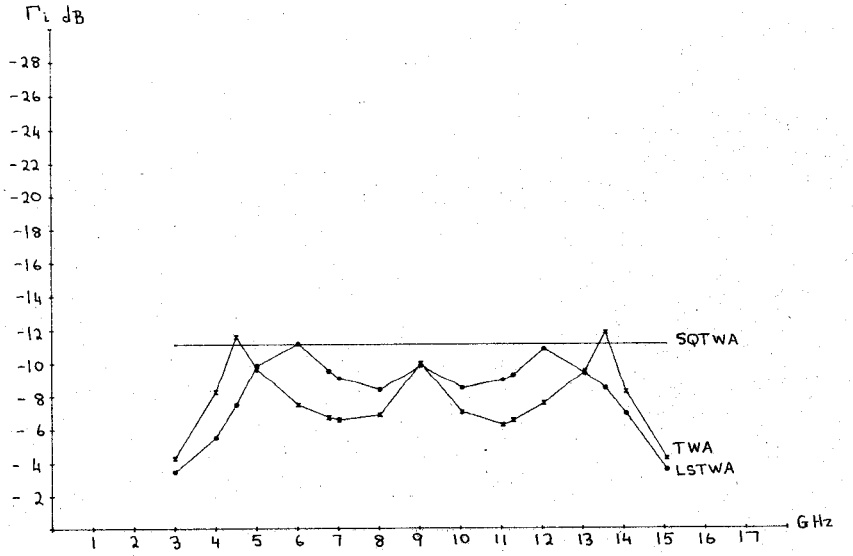


Fig. 4. INPUT port return loss (nonzero-tolerance, ±10 percent, ±20°).

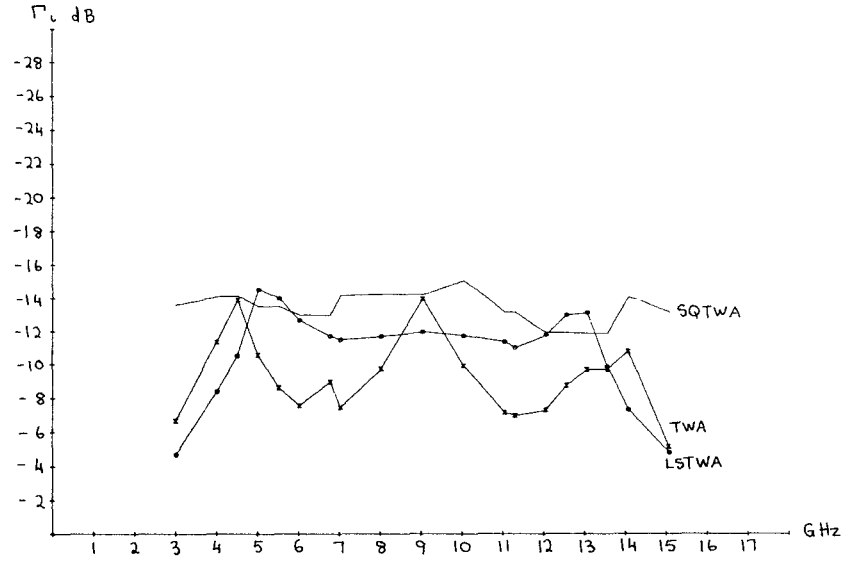


Fig. 5 INPUT port return loss (mismatched case).

TABLE I
FORWARD TRANSMISSION RESULTS

| Case | S Parameter Tolerances | | Combining Loss |
|---|---|---|---|
| | Phase (deg.) | Amp. (%) | (dB) |
| a | 0 | 0 | 0 |
| | ±10 | ±3 | -0.13 |
| | ±20 | ±10 | -0.45 |
| b | ±20 | ±10 | -0.96 |

TABLE II
INPUT PORT RETURN LOSS RESULTS

| Amplifier | Active Device Spread | Passive component Return Loss (dB) | Unsymm. Loss (dB/ ) | Peak INPUT Ret. Loss (dB) | Avail. B.Width @ peak Refl. |
|---|---|---|---|---|---|
| TWA | 0 | | | -11.3 | 4.2 |
| | ±10%, ±10° | | | - 8.2 | 4.4 |
| | ±10%, ±20° | | | - 6.2 | 4.1 |
| | ±10%, ±20° | -15.0 | -1.0 | - 7.0* | 4.7 |
| LSTWA | 0 | | | -19.6 | 2.7 |
| | ±10%, ±10° | | | -12.0 | 2.7 |
| | ±10%, ±20° | | | - 8.2 | 2.8 |
| | ±10%, ±20° | -15.0 | -1.0 | -11.0* | 2.9 |
| SQTWA | 0 | | | *** | ** |
| | ±10%, ±10° | | | -15.0 | ** |
| | ±10%, ±20° | | | -11.0 | ** |
| | ±10%, ±20° | -15.0 | -1.0 | -11.6* | ** |

notes:
* this return loss level is lower because of the loss term
** bandwidth limited to the performance bandwidth of the passive comp.
*** theoretically $\rightarrow -\infty$

### B. INPUT Port Return Loss

The Table II presents comparative results for the simulations described in Section III-B.

Table II indicates that if relatively high $\Gamma_i$ peaks are acceptable, then the TWA offers bandwidths of about 4.3:1 at these values (note that bandwidth is defined as $f_{hi}/f_{low}$). If, however, lower $\Gamma_i$ is required, then the TWA may not be used since these peak $\Gamma_i$ values are not subject to reduction except by increasing the number of elements [4], and even then only modest reductions in peak $\Gamma_i$ are possible. For example, an eight-element TWA exhibits peak $\Gamma_i$ levels of $-12.8$ dB (zero-tolerance case), an improvement of only 1.5 dB.

The LSTWA and SQTWA on the other hand offer the option of achieving arbitrarily low $\Gamma_i$ levels without increasing the number of channels. The bandwidth achievable with the SQTWA is also independent of the number of channels, but in the case of the LSTWA, wider bandwidths necessitate the addition of more channels.

It should be noted that the well-known Lange coupler balanced module is an example of a two-element SQTWA, where the fixed phase shifts are realized using a quadrature coupler.

## V. CONCLUSION

Two new TWA structures have been presented. These devices offer wider port VSWR bandwidths at lower return loss levels than the conventional TWA given the normal $S$-parameter spread of active devices. These improved characteristics allow the use of less uniform active devices, thus increasing yield and lowering costs, enable extremely low VSWR wide-band modules to be realized, which may be cascaded with reduced resultant ripple. Applications may be found in both low- and high-power designs.

## ACKNOWLEDGMENT

The author would like to thank G. Argaman for valuable discussions, and Y. Maor for his programming assistance, as well as the management of RAFAEL (where this work was performed) for the permission to publish. He also thanks the anonymous reviewers for their helpful suggestions.

## REFERENCES

[1] "GaAs FET's from Harris microwave semiconductors," *Microwave J.*, pp 86–87, Oct. 1984.
[2] S. B. Moghe, "Quasi-lumped element impedance matching networks," *Microwave J.*, pp.71–75, Nov. 1981.

[3] J. Goel, "A k-Band GaAs FET amplifier with 8.2 W output power," *IEEE Trans. Microwave Theory Tech.*, vol. MTT-32, pp. 317–323, Mar. 1984.
[4] A. G Bert, D. Kaminsky, and G. Kantorovics, "Progress in GaAs FET power combining with travelling wave combiner amplifiers," *Microwave J.*, pp. 69–72, July 1981.
[5] Y Ayasli, J. L. Vorhaus, R. L. Mozzi, L. D. Reynolds, and R A. Pucel, "A Monolithic GaAs 1-13 GHz travelling wave amplifier," *IEEE Trans. Microwave Theory Tech.*, vol. MTT-30, pp. 976–981, July 1982.
[6] D. J. R. Stock and L J. Kaplan, "A comment on the scattering matrix of cascaded 2N-ports," *IRE Trans. Microwave Theory Tech* , vol. MTT-9, p.454, Sept 1961.
[7] R. S. Elliott, *Antenna Theory and Design*. Englewood Cliffs, NJ: Prentice-Hall, ISBN 0-13-038356-2, 1981, p. 118.
[8] R. S. Elliott, *Antenna Theory and Design*. Englewood Cliffs, NJ. Prentice-Hall, ISBN 0-13-038356-2, 1981, p. 122.
[9] L I. Parad an R. I. Moynihan, "Split-tee power divider," *IEEE Trans. Microwave Theory Tech.*, vol. MTT-13, pp. 91–95, Jan. 1965.
[10] J. Frank, "Bandwidth criteria for phased array antennas," in *Phased Array Antennas*, ed. A. A. Knittel and G. H. Oliner, Aertech House, Lib. Cong Cat. No. 73-189392, 1972, pp. 243–251.
[11] C P. Tresselt, "Broadband tapered line phase shift networks," *IEEE Trans. Microwave Theory Tech.*, vol. MTT-16, pp. 55–52, Jan. 1968.
[12] S B Cohn, "A class of broadband three-port TEM-mode hybrids," *IEEE Trans. Microwave Theory Tech.*, vol. MTT-16, Feb. 1968, pp. 110–116.

# On the Noise Parameters of Isolator and Receiver with Isolator at the Input

MARIAN W. POSPIESZALSKI, SENIOR MEMBER, IEEE

*Abstract* —**Noise parameters of an isolator and those of a receiver with an isolator at the input are reviewed. Some comments on recently published results are offered.**

## I. Introduction

Isolators are very commonly used in low-noise receivers as well as in noise measuring systems (for instance, [1]–[5]). Usually their purpose is to isolate either the noise source or the receiver from the rest of the system. In these cases, the noise properties of either the isolator alone or the receiver with the isolator at the input need to be known. This paper offers a brief discussion of the noise properties of these two-ports and gives closed-form expressions in some idealized cases for the set of noise parameters, namely minimum noise temperature $T_{\min}$, optimum source reflection coefficient $\Gamma_{opt}$, and noise parameter $N$ as defined in [9]. A short discussion of some of the recently published results [4], [5], [11], [15] is also given.

## II. Theory

Consider a linear, noisy system schematically presented in Fig. 1. Signal parameters of both an isolator and a receiver are represented by chain matrices $[A_I]$ and $[A_R]$ and their noise parameters by correlation matrices $[C_{AI}]$ and $[C_{AR}]$, respectively [6]. An isolator is a passive, nonreciprocal, linear two-port with thermal noise generators only and, therefore, its noise parameters can be derived from its signal parameters [7]. The appropriate

Manuscript received June 24, 1985; revised November 12, 1985.
M. W. Pospieszalski is with the National Radio Astronomy Observatory, Charlottesville, VA 22903. The National Radio Astronomy Observatory is operated by Associated Universities, Inc., under contract with the National Science Foundation.
IEEE Log Number 8407183

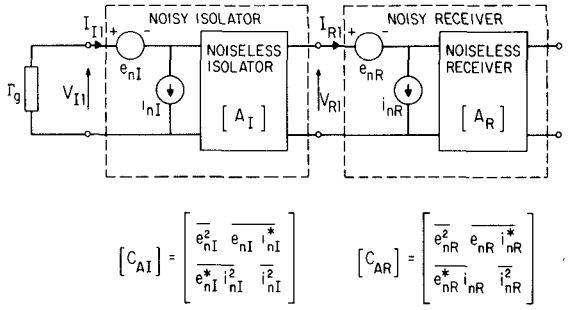


Fig. 1. A cascade connection of isolator and receiver.

equivalent networks with pertinent formulas [7], [8] are given in Fig. 2. Then the correlation matrix $[C_A]$ completely characterizing the noise parameters of the system at the input port of the isolator is [8]

$$[C_A] = [C_{AI}] + [A_I][C_{AR}][A_I]^{\dagger} \tag{1}$$

where the "dagger" designates the complex conjugate of the transpose of $[A_I]$ matrix. Any desired set of noise parameters can be derived from $[C_A]$ (for instance, [6], [8]–[10]).

It should be stressed that this approach is not limited by the particular realization of an isolator as, for instance, a Faraday rotation isolator or an isolator made of a circulator with one port terminated. The noise properties of both isolators are the same if they are at the same physical temperature and their two-port signal parameters are the same.

Although the formulas presented in Figs. 1 and 2 and also (1) lend themselves easily to computer implementation (for instance, [13], [14]), and, therefore, are convenient to use in computer-aided design and/or computer-aided measurement, it is very instructive to discuss the conventional noise parameters of an ideal isolator, which is equivalent to an ideal circulator with one port terminated (Fig. 3(a)). It follows directly from Twiss's [7] general approach or from simple physical reasoning that the noise parameters of an ideal isolator are

$$T_{\min} = 0, \quad \Gamma_{opt} = 0, \quad N = \frac{T_a}{4T_0} \tag{2}$$

where

| | |
|---|---|
| $T_{\min}$ | minimum noise temperature, |
| $\Gamma_{opt}$ | optimum reflection coefficient of the source, |
| $T_0 = 290$ K | standard temperature, |
| $T_a$ | physical temperature of a circulator termination, (or physical temperature of an isolator), |
| $N$ | noise parameter defined in [9]. |

It is instructive to give physical interpretation of the noise parameters given by (2). An ideal isolator emits a noise wave from its input port, which is totally absorbed by the source if $\Gamma_g = \Gamma_{opt} = 0$. In this case, no noise generated by the isolator appears at its output and $T_{\min} = 0$. If $\Gamma_g \neq 0$, part of the noise is reflected back and appears at the isolator output, which gives rise to parameter $N > 0$.

Small losses $L$ of an isolator in the forward direction can be modeled accurately by a cascade connection of an ideal isolator and a matched attenuator, as shown in Fig. 3(b). In this case of a slightly lossy isolator, the noise parameters are

$$T_{\min} = T_a(L-1) \quad \Gamma_{opt=0} \quad N = \frac{T_a + T_{\min}}{4T_0}. \tag{3}$$

0018-9480/86/0400-0451$01.00 ©1986 IEEE